

Supplementary Figures

Impact of the Arctic Oscillation from March on summertime sea ice

Young-Kwon Lim^{1,2*}, Dong L. Wu³, Kyu-Myong Kim³, and Jae N. Lee^{1,3}

¹University of Maryland, Baltimore County, Baltimore, Maryland

²Global Modeling and Assimilation Office (GMAO), NASA Goddard Space Flight Center, Greenbelt, Maryland

³Climate and Radiation Laboratory, NASA Goddard Space Flight Center, Greenbelt, Maryland

* corresponding author

Correspondence to Young-Kwon.Lim@nasa.gov (Young-Kwon Lim)

Revision submitted to Environmental Research Letters

August 25, 2022

Key words: Arctic Oscillation, sea ice, prediction, energy budget, climate variability and change

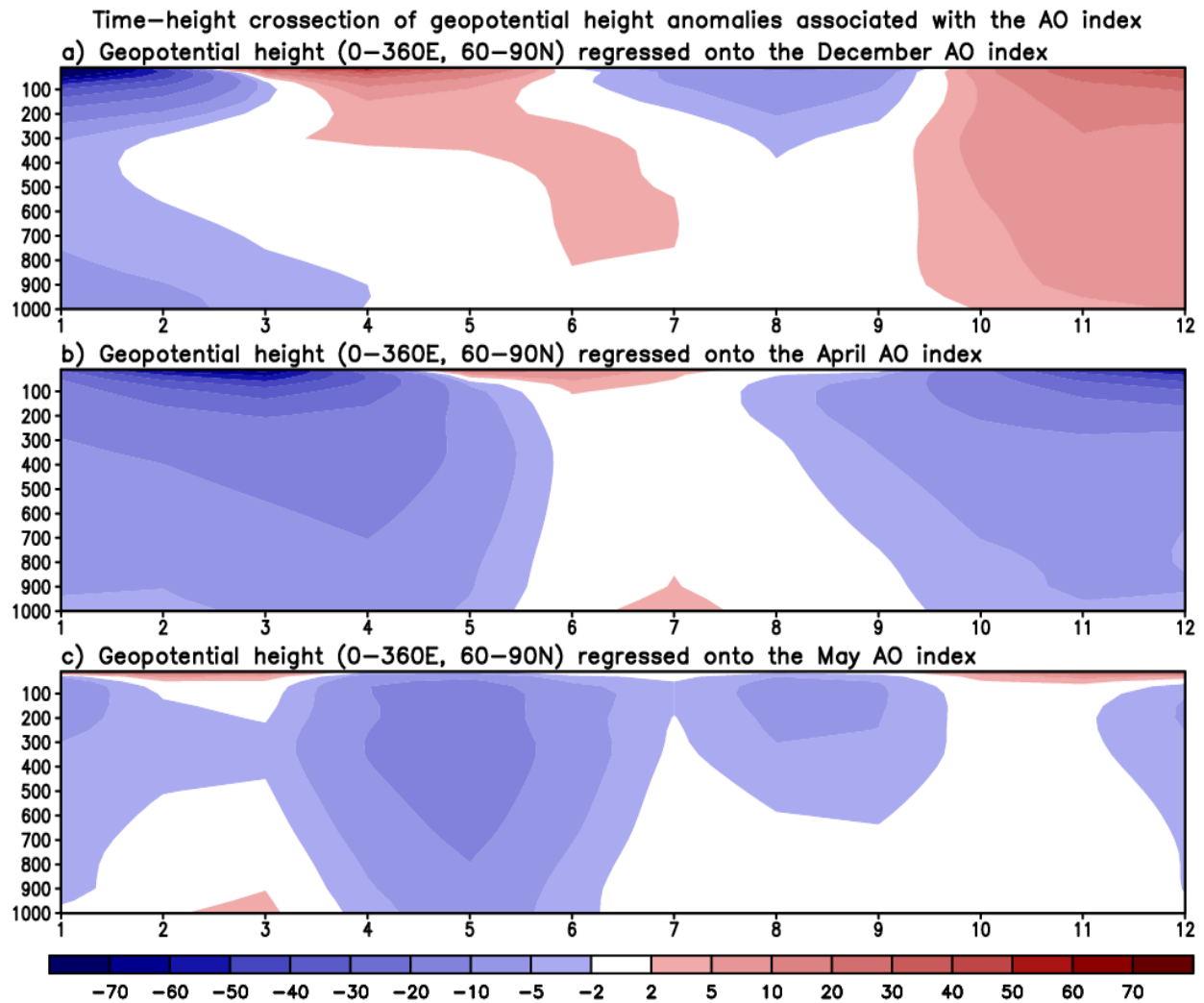


Figure S1. Time-height cross-section of the area-averaged (0° – 360° E, 60° – 90° N) geopotential height anomaly projected onto the AO index in December (upper), April (middle), and May (lower). Time axis represents the months in number and the vertical axis represents the pressure levels in hPa. Unit of the anomaly is m.

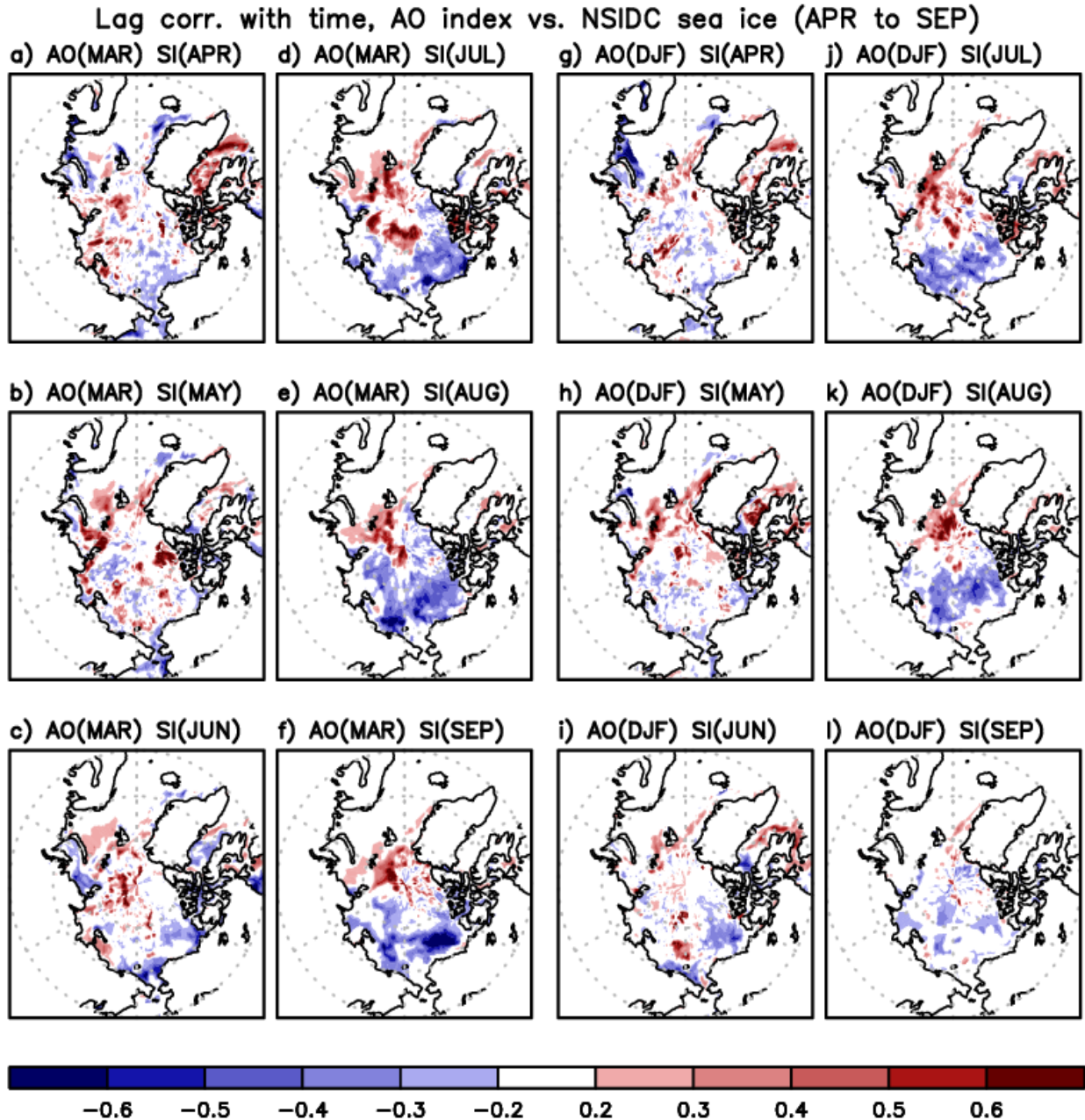
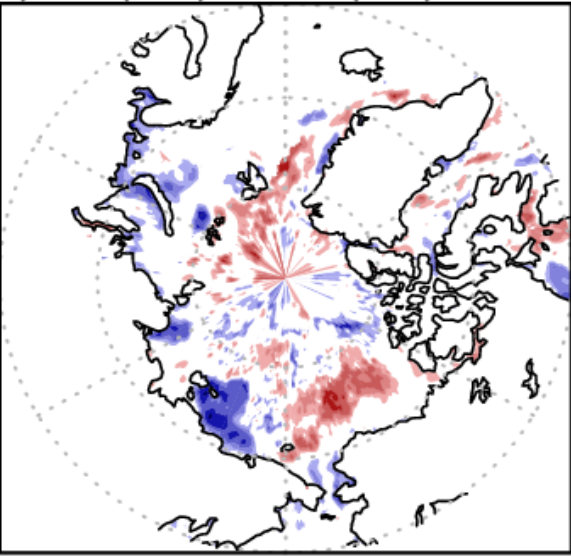


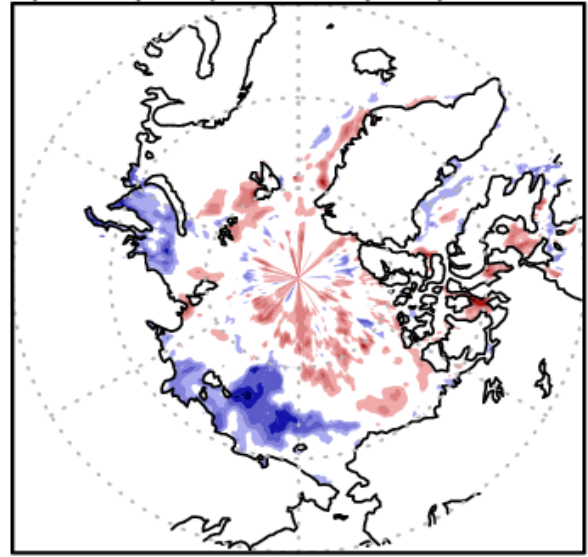
Figure S2. a)-f) Time-lag correlation coefficients of the March AO index in the 21st century (2000-2017) with the NSIDC sea ice concentration anomaly for the following months of a) April, b) May, c) June, d) July, e) August and f) September. g)-l) Same as a)-f) but for the AO index averaged over December through February (with no impact from March).

Lag corr. with time, March AO index vs. NSIDC sea ice (JUN to SEP)

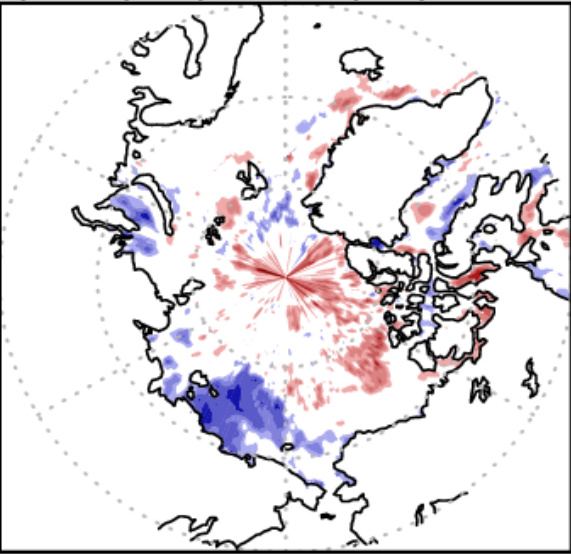
a) AO (MAR) vs. SI (JUN)



c) AO (MAR) vs. SI (AUG)



b) AO (MAR) vs. SI (JUL)



d) AO (MAR) vs. SI (SEP)

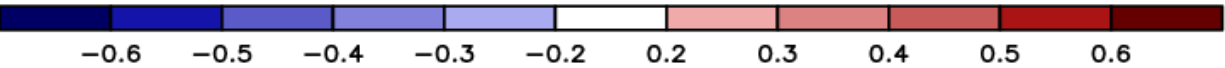
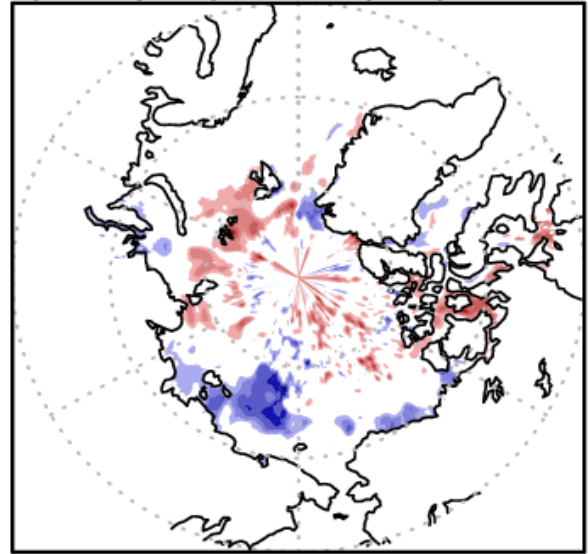


Figure S3. Time-lag correlation coefficients of the March AO index in the 20th century (1980-1999) with the NSIDC sea ice concentration anomaly for the following months of a) June, b) July, c) August and d) September.

Total cloud fraction regressed onto March AO index

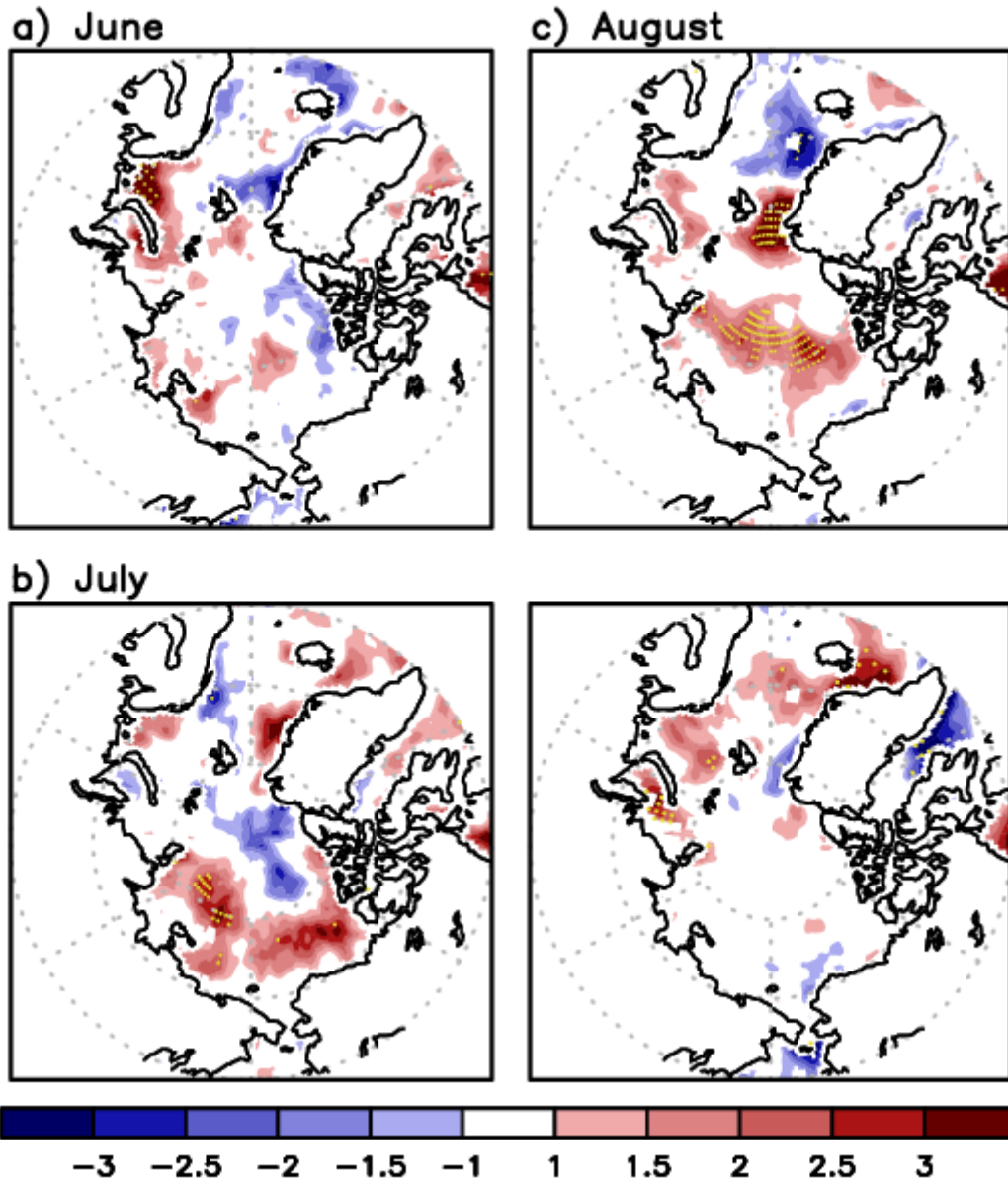


Figure S4. Time evolution of total cloud fraction anomaly from June to September regressed onto the March AO index in the 21st century (2000-2021). Unit is %. Stippling represents the grid points where the total cloud fraction anomaly is significant at 95% confidence.

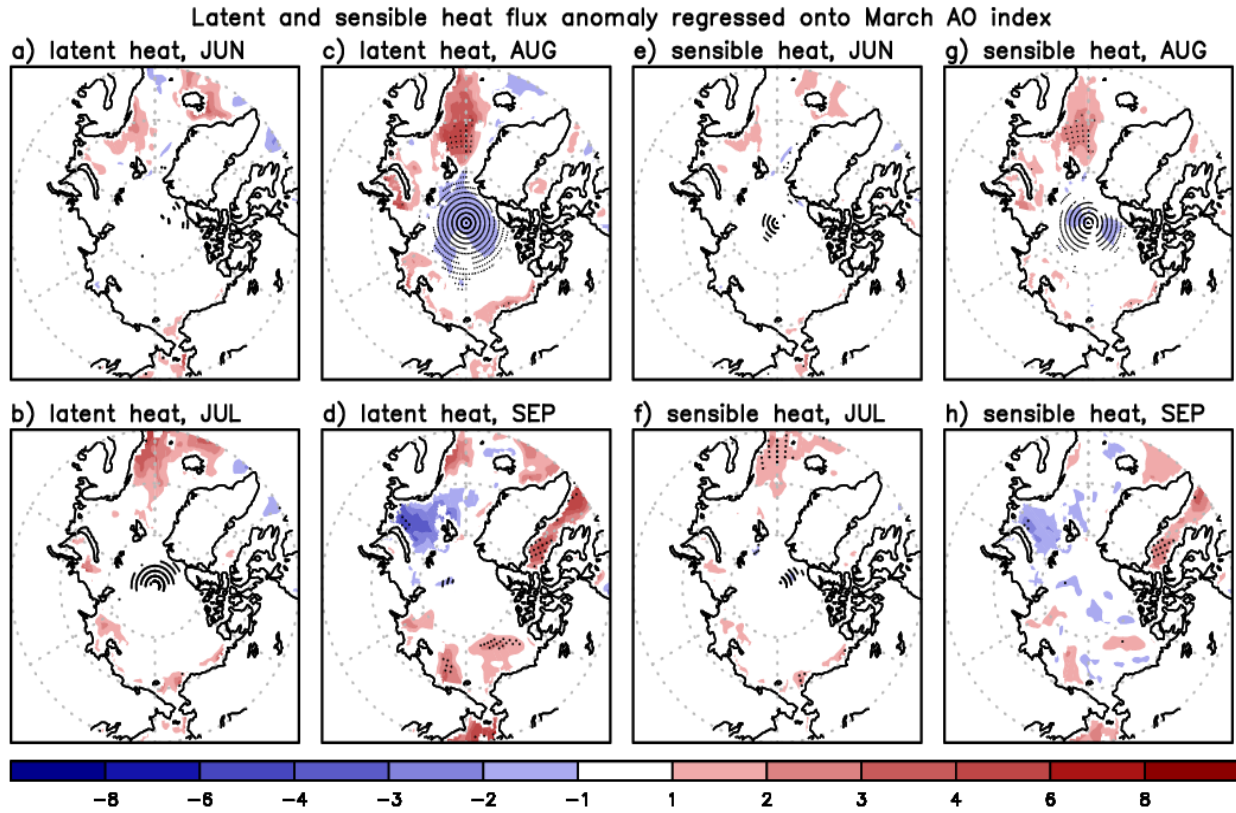


Figure S5. a)-d) Time evolution of the surface latent heat flux anomaly over ocean from June to September regressed onto the March AO index in the 21st century (2000-2021). Unit is W m^{-2} . e)-h) Same as a)-d) but for the sensible heat flux anomaly. Stippling represents the grid points where anomaly is significant at 95% confidence.

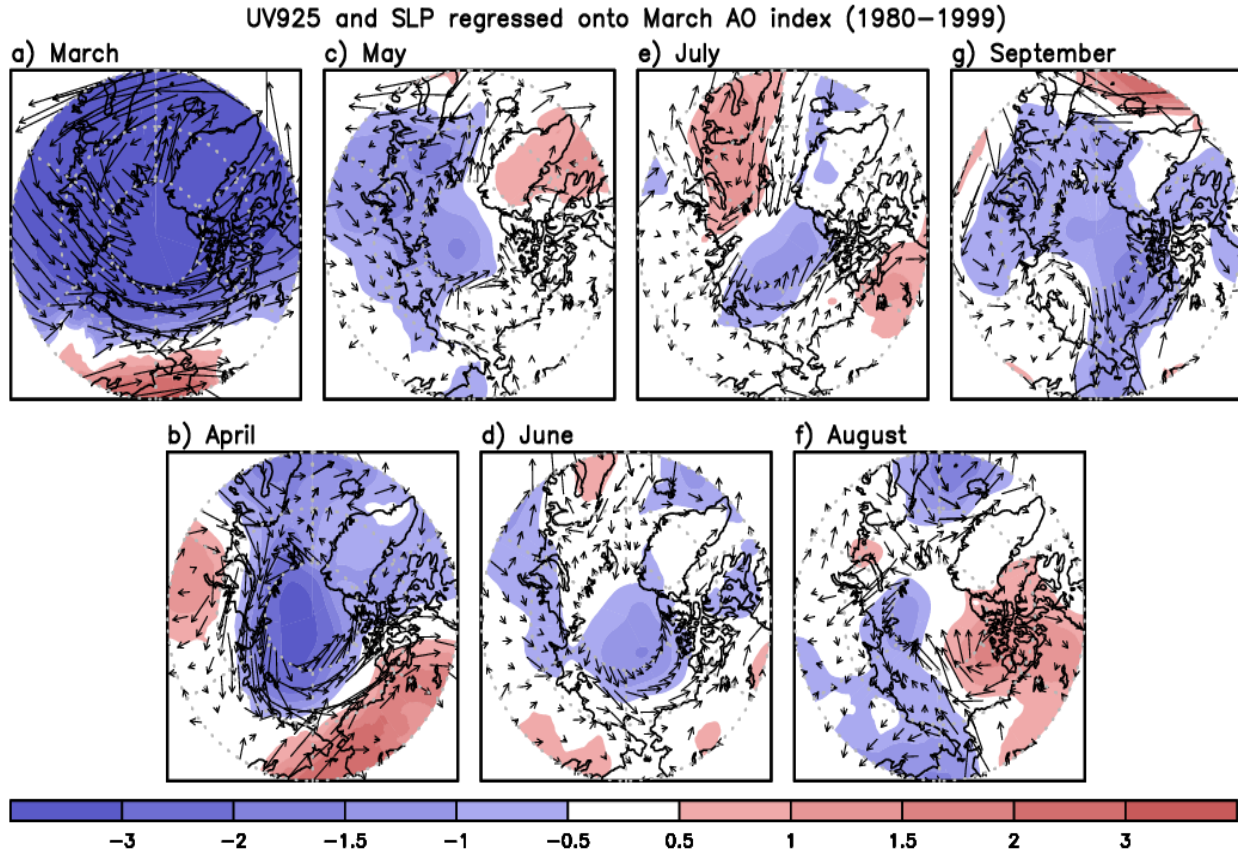


Figure S6. Time evolution of the sea level pressure anomaly (shaded) and horizontal circulation anomaly at 925 hPa level (vectors) from March to September projected onto the March AO index in the 20th century (1980-1999). Unit of the sea level pressure and wind is hPa and m s^{-1} , respectively.

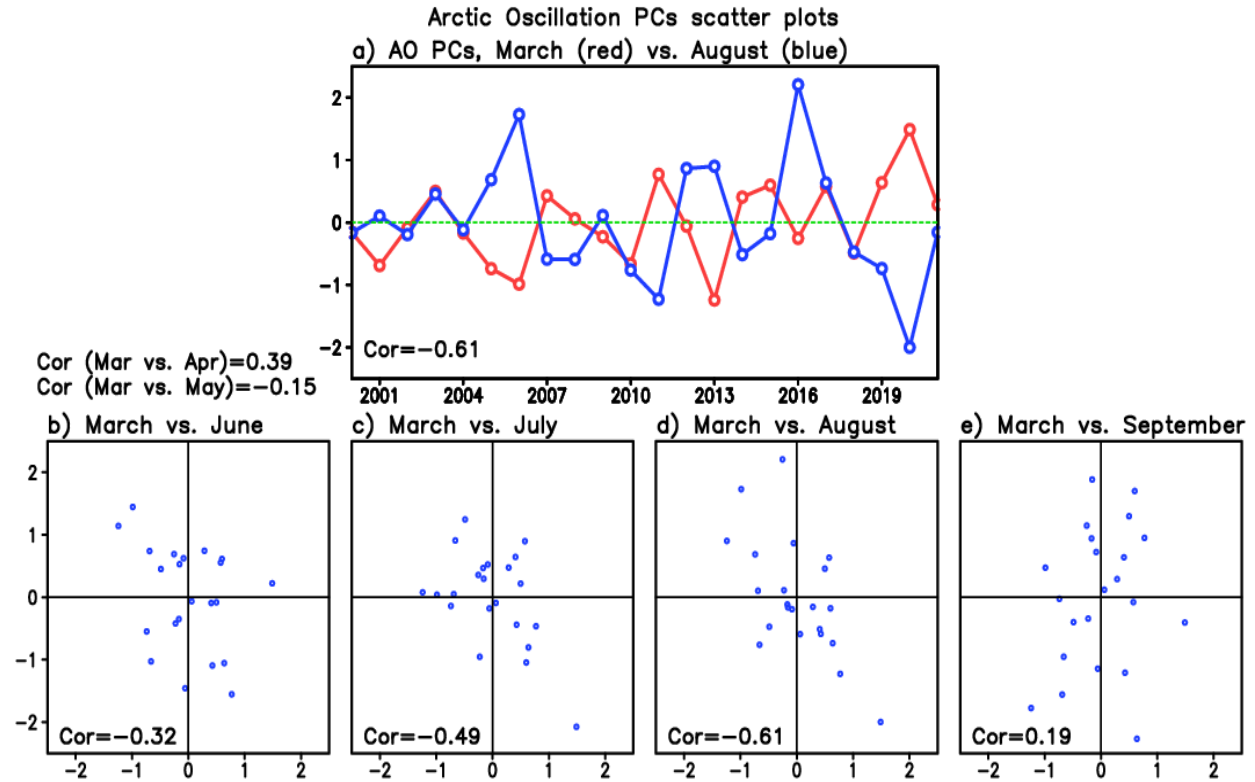


Figure S7. a) Time series of the AO EOF mode for March (red) and August (blue) captured from the MERRA-2 upper-tropospheric (250hPa) geopotential height over the period 2000 to 2021. Correlation of those two time series is provided in the lower-left of the panel a). b)-e) Scatter plots of the AO mode time series between March (x-axis) and b) June, c) July, d) August and e) September. Their correlation coefficients are provided in the lower-left of the panels. Coefficients above the panel b) represent the correlations of the AO mode time series between March and April, and March and May.